COMPARATIVE METHODS OF MEASUREMENT OF CONTACT RESISTIVITY OF METAL-SEMICONDUCTOR CONTACT

Dr. MONISHA CHAKRABORTY

Assistant Professor, School of Bio-Science & Engineering, Jadavpur University, 188, Raja S. C. Mallik Road, Kolkata-700032, India

ABSTRACT

In this paper, comparison of mathematical models to determine contact resistivity of Metal-Semiconductor (M-S) contacts is made. Contact resistivity of M-S contact is obtained using a mathematical model based on the values of ideality factor and barrier height which are obtained from Current–voltage (I-V) characteristics of M-S contact. Contact resistivity of M-S contact is obtained using another mathematical model based on two tuning-parameters. Contact resistivity of M-S contact is also obtained using Shockley's standard Transmission Line Model (TLM) technique. Thin films of $Cd_{1-x}Zn_xTe$ of 1µm thickness for 'x' varying from 0.0567 to 0.2210 are the semiconductor materials fabricated on Nickel coated glass substrates and large work function Nickel is the contact points on these films. I-V characteristic data are recorded from these Ni-$Cd_{1-x}Zn_xTe$ stuctures. The values of contact resistivity of the M-S contacts obtained from these three methods are compared and the results are found to match well.

Keywords - Barrier height, Contact resistivity, Ideality factor, Ni-$Cd_{1-x}Zn_xTe$ structure, Transmission Line Model (TLM), Tuning-parameters.

I. INTRODUCTION

Fabrication of ohmic contact on the surface of semiconducting material is an art rather than science. An ohmic contact between a metal and a semiconductor is defined by the negligible contact resistance relative to bulk and spreading resistance of the semiconductor. To detect ohmicity, there is a standard method, called Transmission Line Model (TLM) measurements, originally proposed by Shockley [1]. Researchers applying TLM, sometimes find that they have to introduce a modified sheet resistance under the M-S contact formed during the annealing/sintering processes and a modified end

resistance in order to fit the theoretical data [1-2]. Another modified method is reported in [3] to determine the value of contact resistivity suitable for both single crystalline and polycrystalline materials. Several other theoretical models and approaches for the extraction of contact resistance of M-S contacts have been proposed previously by other researchers and these are reported in [4-11].

In this paper, contact resistivity of M-S contact is obtained using a mathematical model [5, 7] based on the values of ideality factor and barrier height which are obtained from Current–voltage (I-V) characteristics of the M-S contact. Several approaches to extract diode parameters have been proposed previously and these are reported in [12-14]. In this paper, contact resistivity of Metal-Semiconductor (M-S) contact is also obtained using another mathematical model [10, 15] based on two tuning-parameters. Results obtained from these two methods are compared with the values of contact resistivity of the M-S contacts obtained using TLM measurement technique [1], the standard method of measurement of contact resistivity.

High resistivity II-VI semiconductor compounds e.g. ZnTe, CdTe and their alloys $Cd_{1-x}Zn_xTe$ with stoichiometric value 'x', are the materials of choice for optoelectronic devices [16-20]. Introduction of Zn into CdTe makes the lattice of $Cd_{1-x}Zn_xTe$ tunable, by adjusting the Cd/Zn ratio [21]. The properties of $Cd_{1-x}Zn_xTe$ film vary with the concentration of 'x'. The range of 'x' in $Cd_{1-x}Zn_xTe$ thin film lies preferably within $0.05 \le$ 'x' ≤ 0.95 [22, 31]. Some studies on the structural and optical properties of II-VI compound semiconductors are proposed previously and these are reported in [24-33]. Designable semiconductor bandgap is helpful for controlling the resistivity as well as the valence band and conduction band alignment at the semiconductor interface. Cadmium Zinc Telluride (CZT) is a radiation detector material that provides new functionality and improved performance in single-photon emission computed tomography (SPECT) [34-

[35]. CdTe/CZT-based surgery probes have large impact on patient management in surgical oncology. Excellent large-field of view modules have already been realized as reported in [36]. But CZT suffers from ohmic contact problems because of its high electron affinity and large work function. Nickel has large work function [37-38] and the possibility of Nickel to match with CZT has been reported in [38]. A group of researchers has reported in [39] formation of stable ohmic contact to CdTe thin films. Some other methods of forming low resistance contacts on p-CdTe are reported in [40-42]. In the present work, $Cd_{1-x}Zn_xTe$ thin films of 1µm thickness for 'x' varying from 0.0567 to 0.2210 are chosen as the semiconducting materials and Nickel is chosen as the top and bottom contacts for these fabricated films.

In this work, proper methods are adopted to fabricate $Cd_{1-x}Zn_xTe$ thin films of 1µm thickness and these are discussed in section II of this paper. The mathematical calculation for obtaining 'x' is discussed in section III of this paper. TLM measurements to determine contact resistivity of M-S contact is discussed in section IV of this paper. The mathematical model [5, 7] to obtain contact resistivity of M-S contact based on the values of ideality factor and barrier height which are obtained from Current–voltage (I-V) characteristics of the M-S contact is discussed in section V of this paper. The mathematical model based on tuning-parameters [10, 15] to obtain contact resistivity of M-S contact is discussed in section VI of this paper. Results obtained from these three methods for the fabricated $Ni-Cd_{1-x}Zn_xTe$ structures are discussed in section VII of this paper. The significance of the results of this work is discussed in section VIII of this paper. The work is concluded in section IX of this paper.

II. MATERIALS AND METHODS

In this work, physical deposition method is adopted to fabricate six large area $Cd_{1-x}Zn_xTe$ thin films of 1µm thickness. Surface cleaning of the substrate has predominant effect on the growth of the film on it. Thus prior to deposition, glass substrates are carefully cleaned. Commercially available glass slides of dimensions 23 mm x 37 mm x 1 mm are dipped in chromic acid for 2 hours. These are washed with detergent and finally ultrasonically cleaned with acetone before use.

In order to design the six different compositions of $Cd_{1-x}Zn_xTe$ 1µm thin films, six different % ratio of the stack layer of ZnTe/CdTe is chosen and these are 20:80, 30:70, 40:60, 50:50,

60:40 and 70:30. For these six ratios of the stack layer of ZnTe/CdTe, six different values of 'x' are obtained. The mathematical detail is discussed with a sample calculation in section III of this paper.

For the film fabrication, 500W RF Sputtering unit has been used. ZnTe and CdTe targets are placed in the target holders of the RF sputtering unit. Ni-coated glass substrates are kept at the bottom of the target holder and temperature to the order of 100°C is maintained on the substrates. Argon gas is injected from outside and pressure of the order of 10^{-2} Torr has been maintained. At this pressure, the RF unit is energized and a power of 500W with a frequency of 13.56 MHz is applied between the target and the substrate. On application of this RF power the target gets energized and vapour of the target material produced deposits on the substrate. At the substrate temperature the film gets crystallized and the thickness is dependent on the sputtering time. Both CdTe and ZnTe targets are sputtered sequentially and a stack layer of ZnTe/CdTe is thus obtained. The stack layer is then annealed in vacuum (10^{-5} Torr) for an hour at 300°C. Both Cadmium and Zinc tried to inter-diffuse among each other to get into a stabilized state. Applications of thermal energy initiate both cadmium and zinc inter-diffusion. However, the stoichiometric ratio of cadmium and zinc is not equal and as a result the film is formed in the form of $Cd_{1-x}Zn_xTe$. The value of 'x' decides whether the film is CdTe or ZnTe. Thickness and deposition time for CdTe and ZnTe layers for each composition of $Cd_{1-x}Zn_xTe$ films of 1µm thickness are tabulated in Table 1.

Circular dots of 2 mm diameter of Nickel are deposited by Vacuum Evaporation technique onto the films. The contacts are then annealed for half an hour in vacuum (10^{-5} Torr) at 100°C. The layered structure of the fabricated film for I-V characteristics studies is shown in Fig. 1.
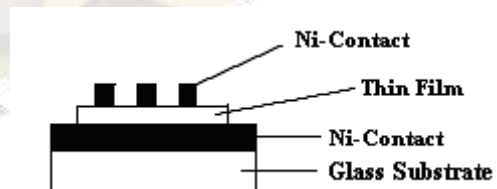

Fig. 1 Metal-Semiconductor structure for I-V characteristic studies

III. SAMPLE CALCULATION OF 'X'

In this section, the mathematics to determine 'x' in $Cd_{1-x}Zn_xTe$ thin film is discussed with a sample

calculation. For this purpose, one out of the six samples is considered and this is a 1µm stack of CZT comprised of ZnTe film deposited on CdTe film. Percentage thickness ratio of ZnTe : CdTe layer is 60:40 and this can be expressed as given in Eq. (1.1).

$$\frac{\% ZnTe}{\% CdTe} = \frac{60}{40} = \frac{n_{ZnTe}}{n_{CdTe}} = \frac{\dfrac{m_{ZnTe}}{M_{ZnTe}}}{\dfrac{m_{CdTe}}{M_{CdTe}}} \qquad (1.1)$$

where,
m_{ZnTe} and m_{CdTe} are the masses of ZnTe and CdTe layers respectively to attain the % ratio ZnTe : CdTe as 60:40.
M_{ZnTe} and M_{CdTe} are the molar masses of ZnTe and CdTe respectively and these values are M_{ZnTe} =193 gms/mol and M_{CdTe}=240 gms/mol. On putting these values, Eq. (1.1) becomes,

$$1.5 = \frac{\rho_{ZnTe}.T_{ZnTe}.A.240}{\rho_{CdTe}.T_{CdTe}.A.193} \qquad (1.2)$$

where,
'A' is the cross-sectional area of the substrate. ρ_{ZnTe} and ρ_{CdTe} are the density of ZnTe and CdTe layers respectively and these values are ρ_{ZnTe} = 6.34 gms/cc and ρ_{CdTe}=5.85 gms/cc. T_{ZnTe} and T_{CdTe} are the values of thickness of ZnTe and CdTe layers respectively. On putting these values, Eq. (1.2) becomes,

$$\frac{T_{ZnTe}}{T_{CdTe}} = 1.113022477 \qquad (1.3)$$

$$T_{ZnTe} + T_{CdTe} = 1\mu m \qquad (1.4)$$

Solution of Eq. (1.3) and Eq. (1.4) gives the values of the thickness of CdTe and ZnTe layers and these are,
T_{CdTe} = 473.26 nm and T_{ZnTe} = 526.74 nm.   (1.5 a)
Deposition rates for CdTe and ZnTe targets are 78 nm/min and 45 nm/min respectively.   (1.5 b)
From Eq. (1.5 a) and Eq. (1.5 b) the deposition times for CdTe and ZnTe layers for this sample are obtained and these values are t_{CdTe} = 6 mins 4 sec and t_{ZnTe} = 11 mins 42 sec respectively.   (1.5 c)
So, mass of ZnTe layer, m_{ZnTe} = 3339.53.A.10^{-7} gms and mass of CdTe layer, m_{CdTe} = 2768.57.A.10^{-7} gms.
Molar mass of Zinc, M_{Zn} = 65.38 gms/mol.
So, 1139.29.A.10^{-7} gms of zinc is present in 3339.53.A.10^{-7} gms of ZnTe.
∴ Fraction of zinc in this CZT matrix

$$= \frac{1139.29.A.10^{-7}}{(2768.57 + 3339.53).A.10^{-7}} = 0.1865 \qquad (1.6)$$

Similarly, for other % ratios of ZnTe : CdTe layers considered in this study, the values of 'x' are calculated and these results are tabulated in Table 1.

IV. MEASUREMENT OF CONTACT RESISTIVITY

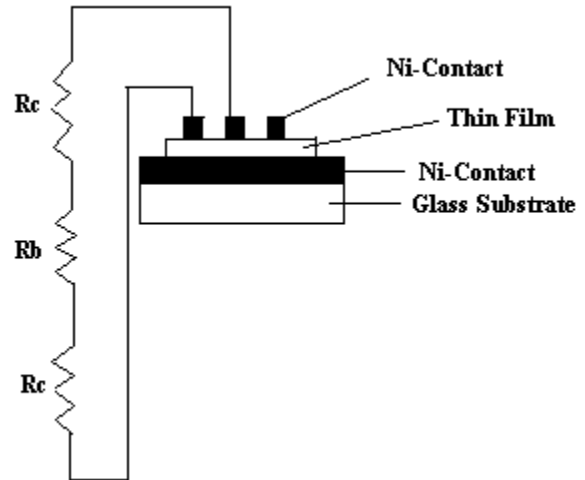Measurement of contact resistivity of M-S contact using TLM model is shown in Fig. 2.

Fig. 2 Method for measuring contact resistivity

The total resistance R_t is given in Eq. (1.7)
$R_t = R_c + R_b + R_c$ (1.7)
Where, Rc is contact resistance and Rb is bulk resistance
Eq. (1.7) can be written as given in Eq. (1.8)

$$R_t = 2\frac{\rho_c}{A_{eff}} + \rho_b \frac{l}{A_b} \qquad (1.8)$$

with ρ_c as contact resistivity and ρ_b as bulk resistivity,

A_{eff} is cross-sectional area of contact=$\pi \dfrac{d^2}{4}$, d = 2mm = diameter of the metallic contact
A_b = t.d, t = thickness of the semiconductor film
The plot of l vs R_t is an equation of a straight line with $\dfrac{\rho_b}{td}$ as the slope and $\dfrac{\rho_c}{A_c}$ as intercept. From this plot the values of ρ_c and ρ_b are evaluated.

V. MATHEMATICAL MODEL-1

Contact resistivity of M-S contact obtained using the mathematical model [5, 7], based on the values of ideality factor and barrier height which is obtained from Current–voltage (I-V) characteristics of the M-S contact is briefly mentioned here.

Contact resistivity (ρ_c) is given by,

$$\rho_c = \left(\frac{dV}{dJ}\right)_{V=0} \qquad (1.9)$$

Normally, the J-V relationship of a rectifying contact is represented by

$$J = J_0[\exp(\frac{qV}{nKT})-1] \qquad (1.10)$$

with V as applied voltage, Jo as reverse saturation current density, A_{eff} as effective area of M-S contact, n as ideality factor [37], T as absolute temperature (300 K), K as Boltzmann Constant [37]. Taking only the linear terms, and from Eq. (1.9) and Eq. (1.10),

$$\rho_c = \left(\frac{Aeff.n.K.T}{Io.q}\right) \qquad (1.11)$$

Considering that the conduction has taken place at the metal-semiconductor interface due to thermionic emission phenomenon then,

$$I_0 = Aeff.A^*.T^2.\exp\left(-\frac{q\phi_b}{kT}\right) \qquad (1.12)$$

with ϕ_b as potential barrier at the metal-semiconductor interface and A^* as Richardson's constant= $1.20173*10^6 Am^{-2}K^{-2}$. From Eq. (1.11) and Eq. (1.12),

$$\rho_c = \left(\frac{K.\exp\left(\frac{q\phi_b}{kT}\right)}{q.A.T}\right) \qquad (1.13)$$

Where, $A = \left(\frac{A^*}{n}\right)$, $\qquad (1.14)$

ρ_c is evaluated using Eq.(1.13) where, n and ϕ_b are calculated using the theoretical formulation reported in [2] and it is briefly mentioned here.

In the equilibrium condition of a metal-semiconductor contact, the total current density (J) becomes,

$$J = J_0\left[\exp\left(\frac{qV_d}{nkT}\right)-1\right] \qquad (1.15)$$

Where $V_d = V - JA_{eff}R_s$ and A_{eff} & R_s are the effective contact area and series resistance of the metal-semiconductor contact respectively.

J is the sum of two current components – from the semiconductor to the metal ($J_{S \to M}$) and from the metal to the semiconductor ($J_{M \to S}$), where

$$J_{S \to M} = J_0 \exp\left(\frac{qV_d}{nkT}\right)$$

and $\qquad J_{M \to S} = J_0$

Here $\qquad J_0 = A^*T^2 \exp\left(-\frac{q\phi_b}{kT}\right) \qquad (1.15a)$

At large forward bias ($V_d>3kT/q$), Eq.(1.15) reduces to,

$$J = J_0\left[\exp\left(\frac{qV_d}{nkT}\right)\right] \qquad (1.15b)$$

On substituting the expression for V_d, Eq. (1.15b) becomes;

$$V = \frac{n}{\beta}\ln\left(\frac{J}{J_0}\right) + JA_{eff}R_s \qquad (1.16)$$

Where, $\beta = \frac{q}{kT}$

Substitution of J_0 from Eq. (1.15a) in Eq. (1.16) gives,

$$V = JA_{eff}R_s + n\phi_b + \frac{n}{\beta}\ln\left(\frac{J}{A^*T^2}\right) \qquad (1.17)$$

On differentiating V with respect to J, Eq. (1.17) reduces to,

$$\frac{dV}{dJ} = A_{eff}R_s + \frac{1}{J}\frac{n}{\beta} \qquad (1.18)$$

The term $\frac{dV}{dJ} = R_D$, the dynamic resistance of the barrier.

A plot of R_D vs $\frac{1}{J}$ of Eq. (1.18) bears a straight line with $A_{eff}.R_s$ as the intercept and $\frac{n}{\beta}$ as the slope.

Again Eq. (1.17) can be rewritten as,

$$H(V) = JA_{eff}R_s + n\phi_b \qquad (1.19)$$

Where $\quad H(V) = V - \dfrac{n}{\beta} \ln\left(\dfrac{J}{A^*T^2}\right) \quad$ (1.19a)

The values of H(V) can be evaluated by substituting values of J with corresponding values of V. Again the plot of H(V) vs. J bears a straight line with $A_{eff}R_s$ as the slope and $n\phi_b$ as intercept. From the above two plots the values of n and ϕ_b are evaluated.

VI. MATHEMATICAL MODEL-2

Contact resistivity of M-S contact obtained using the mathematical model [10, 15], based on two tuning-parameters is briefly mentioned here. The mathematical model for current in M-S contact is given in Eq. (1.20)

$$I = a.V^b \qquad (1.20)$$

with 'V' as applied voltage, 'I' as current, 'a' and 'b' as the tuning-parameters. Measurements are done at room temperature of 27°C. From Eq. (1.20) it is seen that when b = 1, the contact is ohmic or non-injecting and $\dfrac{1}{a}$ represents resistance, which will be very small in that case with $I = J.A_{eff}$, with J as Current density and A_{eff} as effective area of M-S contact. This implies that the extent of ohmicity of a M-S contact depends on the value of 'b' which is related to 'a'. As 'b' approaches 1, the contact tends to be more ohmic. Eq. (1.20) can be written as,

$$V = \left(\dfrac{J.A_{eff}}{a}\right)^{\frac{1}{b}} \qquad (1.21)$$

Therefore, $\ln(V) = \dfrac{1}{b}\ln(J) + \dfrac{1}{b}\ln(\dfrac{A_{eff}}{a}) \qquad$ (1.22)

Eq. (1.22) so obtained is the equation of a straight line. The plot of $\ln(V)$ vs $\ln(J)$ gives $\dfrac{1}{b}\ln(\dfrac{A_{eff}}{a})$ as the intercept and $\dfrac{1}{b}$ as the slope.

.   From the above plot, the values of slope and intercept are obtained and from these, the values of the tuning parameters 'a' and 'b' for the M-S contacts are evaluated.

In general, the formation of electrical contact is defined in terms of contact resistivity (ρ_c) whose value should be very low in case of an ohmic contact. The expression for ρ_c is given by,

$$\rho_c = \left(\dfrac{dV}{dJ}\right)_{V=0} \qquad (1.23)$$

On differentiating V with respect to J, Eq. (1.22) becomes,

$$\dfrac{dV}{dJ} = \dfrac{V}{b.J} \qquad (1.24)$$

The expression of 'V' from Eq. (1.21) is put in Eq. (1.24) and this gives Eq. (1.25),

$$\rho_c = \dfrac{A_{eff}}{b.I}\left(\dfrac{I}{a}\right)^{\frac{1}{b}}\Bigg|_{V=0} \qquad (1.25)$$

Contact resistivity ρ_c is evaluated using Eq. (1.25).

VII. RESULTS

Current-Voltage (I-V) characteristic data are recorded for the six Ni-Cd$_{1-x}$Zn$_x$Te structures for 'x' varying from 0.0567 to 0.2210 using Keithley (Model No. 2440) 5A Source meter at room temperature of 27°C. For mathematical model-1, plots of R$_D$ vs 1/J are obtained for these Ni-Cd$_{1-x}$Zn$_x$Te structures and the values of ideality factors (n) for these Ni-Cd$_{1-x}$Zn$_x$Te structures are calculated as discussed in section V of this paper. Plots of H(V) vs. J are obtained for all these Ni-Cd$_{1-x}$Zn$_x$Te structures and the values of barrier heights (Φ_b) for these Ni-Cd$_{1-x}$Zn$_x$Te structures are calculated as discussed in section V of this paper. Substituting the values of 'n' and 'Φ_b' in Eq. (1.13), contact resistivity of these Ni-Cd$_{1-x}$Zn$_x$Te structures are evaluated. The normalized values of ideality factor, barrier height and contact resistivity of these Ni-Cd$_{1-x}$Zn$_x$Te structures obtained using Mathematical Model-1 are tabulated in Table 2. For mathematical model-2, I-V data of these Ni-Cd$_{1-x}$Zn$_x$Te structures are put in Eq. (1.22). Plots of ln(V) vs ln(J) are obtained for all the six Ni-Cd$_{1-x}$Zn$_x$Te structures and the values of tuning parameters 'a' and 'b' for these samples are calculated as discussed in section VI of this paper. Substituting the values of 'a' and 'b' in Eq. (1.25), contact resistivity of these Ni-Cd$_{1-x}$Zn$_x$Te structures are evaluated. The normalized values of tuning-parameters and contact resistivity of these Ni-Cd$_{1-x}$Zn$_x$Te structures obtained using Mathematical Model-2 are tabulated in Table 2. The effective area of these Ni-Cd$_{1-x}$Zn$_x$Te structures is 0.0314 cm^2. Current-Voltage (I-V) characteristic plot recorded using Keithley-2440, 5A Source meter, for Ni-Cd$_{1-x}$Zn$_x$Te structure at 'x' = 0.1865, is shown in Fig. 3 as sample result.
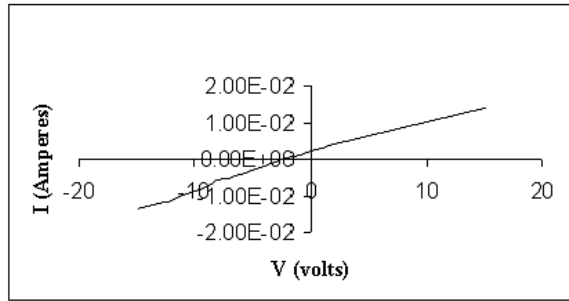
Fig. 3 Current-Voltage characteristic plot of Ni-Cd$_{1-x}$Zn$_x$Te structure at 'x' = 0.1865

Out of the six compositions, ideality factor for Ni-Cd$_{1-x}$Zn$_x$Te structure at 'x' = 0.1182 is found to be maximum and the values of ideality factors for all the six samples are divided by this maximum value and this normalized dataset is tabulated in Table 2. Similarly, out of the six compositions of Ni-Cd$_{1-x}$Zn$_x$Te structure, the value of the barrier height is found to be maximum at 'x' = 0.0870 and the values of barrier heights for all the six samples are divided by this maximum value and this normalized dataset is tabulated in Table 2. Out of the six compositions, the tuning parameter 'a' for Ni-Cd$_{1-x}$Zn$_x$Te structure at 'x' = 0.1865 is found to be maximum and the values of the tuning parameter 'a' for all the six samples are divided by this maximum value and this normalized dataset is tabulated in Table 2. Similarly, out of the six compositions, the tuning parameter 'b' for Ni-Cd$_{1-x}$Zn$_x$Te structure at 'x' = 0.0567 is found to be maximum and the values of the tuning parameter 'b' for all the six samples are divided by this maximum value and this normalized dataset is tabulated in Table 2. The values of contact resistivity obtained using Mathematical Model-1 for all the Ni-Cd$_{1-x}$Zn$_x$Te structures considered in this work are normalized with respect to the value of contact resistivity obtained using Mathematical Model-1 for Ni-Cd$_{1-x}$Zn$_x$Te structure at 'x' = 0.1510. Similarly, the values of contact resistivity obtained using Mathematical Model-2 for all the Ni-Cd$_{1-x}$Zn$_x$Te structures considered in this work are normalized with respect to the value of contact resistivity obtained using Mathematical Model-2 for Ni-Cd$_{1-x}$Zn$_x$Te structure at 'x' = 0.1510. Similarly, the values of contact resistivity obtained using TLM Model for all the Ni-Cd$_{1-x}$Zn$_x$Te structures considered in this work are normalized with respect to the value of contact resistivity obtained using TLM Model for Ni-Cd$_{1-x}$Zn$_x$Te structure at 'x' = 0.1510. From the results as quoted in Table 2, it is observed that the results obtained from the three methods are in good agreement amongst each other.

VIII. DISCUSSIONS

Results of this paper reveal that Mathematical Model-1 for measurement of contact resistivity of M-S contact based on the values of ideality factor and barrier height, which are obtained from the Current – Voltage (I-V) characteristic data of M-S contact has worked well and it has given results which are in good agreement with the results obtained using standard TLM model for measurement of contact resistivity of M-S contacts. The Mathematical Model-2 for measurement of contact resistivity of M-S contact based on tuning - parameters have illuminated some of the novel features in understanding both injecting and non-injecting phenomena in M-S contact. The role of the tuning parameters, 'a' and 'b' in deciding whether a M-S contact is injecting or non-injecting has been discussed in section VI of this paper. Results obtained from Mathematical Model-2 are also found to be in good agreement with the results obtained using standard TLM model for measurement of contact resistivity of M-S contacts. From Table 2, it is evident that ideality factor, barrier height and the two tuning -parameters 'a' and 'b' of M-S contacts are functions 'x'. Results obtained from the three models for the measurement of contact resistivity of M-S contacts, as quoted in Table 2, indicate that the lowest value of contact resistivity is obtained for Ni-Cd$_{1-x}$Zn$_x$Te structure at 'x' = 0.1865. Results of this paper also indicate that Mathematical Model-1 and Mathematical model-2, as discussed in section V and section VI of this paper respectively, can be considered as alternative models for measurement of contact resistivity of M-S contacts.

IX. CONCLUSION

This study infers that contact resistivity of Ni-Cd$_{1-x}$Zn$_x$Te structures for 'x' varying from 0.0567 to 0.2210, obtained from the three models considered in this work, are in close agreement amongst each other. The results of the three models confirm that Ni-Cd$_{1-x}$Zn$_x$Te structure at 'x' = 0.1865 is the best M-S contact with respect to its lowest value of contact resistivity.

Table 1 Thickness and Deposition Times of ZnTe and CdTe layers in 1µm CZT Films

S..No.	(%ZnTe): (%CdTe)	Thickness of ZnTe layer T_{ZnTe} (nm)	Thickness of CdTe layer T_{CdTe} (nm)	Deposition time of CdTe layer t_{CdTe}	Deposition time of ZnTe layer t_{ZnTe}	Fraction of Zinc in CZT matrix, 'x'
1	20:80	156.48	843.52	10 mins 49 sec	3 mins 29 sec	0.0567
2	30:70	241.29	758.71	9 mins 44 sec	5 mins 22 sec	0.0870
3	40:60	330.97	669.03	8 mins 35 sec	7 mins 21 sec	0.1182
4	50:50	425.95	574.05	7 mins 22 sec	9 mins 28 sec	0.1510
5	60:40	526.74	473.26	6 mins 4 sec	11 mins 42 sec	0.1865
6	70:30	633.88	366.12	4 mins 42 sec	14 mins 5 sec	0.2210

Table 2: Normalized values of ideality factor, barrier height, tuning-parameters and contact resistivity of Ni-$Cd_{1-x}Zn_xTe$ structures

S. No.	Fraction of Zinc in CZT matrix ('x')	Ideality factor	Barrier height	Tuning Parameter 'a'	Tuning Parameter 'b'	Contact Resistivity, (Using Mathematical Model-1)	Contact Resistivity (Using Mathematical Model-2)	Contact Resistivity (Using TLM Model)
1	0.0567	0.3106	0.9582	0.1290	1.0000	0.3744	0.2936	0.3513
2	0.0870	0.1309	1	0.2504	0.4725	0.4309	0.4860	0.4142
3	0.1182	1.0000	0.8923	0.3178	0.5314	0.2472	0.3490	0.3700
4	0.1510	0.6578	0.9679	0.1044	0.6637	1.0000	1.0000	1.0000
5	0.1865	0.3778	0.9164	1.0000	0.3894	0.1667	0.1874	0.1887
6	0.2210	0.1706	1	0.2589	0.4477	0.5617	0.5805	0.5391

REFERENCES

[1]. B. Ghosh, M. J. Carter, R. W. Miles, R. Hill, Electr. Lett. 29 (5), 1993, 438-440.

[2]. B. Ghosh, D. Sc. Engg thesis, Jadavpur University, Kolkata, India, 2006.

[3]. W. Schocley, Research and investigations of inverse epitaxial UHF power transistor, Report No. AL-TOR-64-207, Air Force Atomic Laboratory, Wright-Patterson Air Force Base, Ohio, 1964.

[4]. B. Ghosh, Journal of Microelectronics Engineering, 86, 2009, 2187-2206.

[5]. M. Chakraborty, International Journal of Engineering Science and Technology, 3(7), 2011, 5956-5963.

[6]. V. V. Filippov, P. V. Frolov, N. N. Polyakov, Russian Physics. 46, 2005, 726-735.

[7]. M. Chakraborty, International Journal of Engineering Research and Applications, 1(3), 2011, 1017-1025.

[8]. G. P. Carvar, J. J. Kopanski, D. B. Novotny, R. A. Forman, IEEE Transactions on Electron Devices. 35, 1988, 489-497.

[9]. B. Ghosh, R. W. Miles, and M. J. Carter, Electronic Letters, 32(10), 1996, 932-933.

[10]. M. Chakraborty, International Journal of Engineering Science and Technology, 3(6), 2011, 4794-4800.

[11]. S. Averine, Y. C. Chan, and Y. L. Lam, Applied Physics Letters. 77(2), 2000, 274-276.

[12]. S. K. Cheung, N. W. Cheung, Applied Physics Lett. 49 (2), 1986.

[13]. H. Bayhan, A. S. Kavasoglu, Turk J Phys, 31, 2007, 7-10.

[14]. K. W. Boer, Journal of Applied Physics, 51(8), 1980, 4518-4522.

[15]. M. Chakraborty, International Journal of Engineering Science and Technology, 3(8), 2011, 6299-6304.

[16]. J. P. Faurie, J. Reno, and M. Boukerche, J. Crystal Growth, 72, 1985, 111.

[17]. R. Dornhaus, G. Nimitz, G. Höhler , and E. A. Nickisch, Springer, 1983, 119.

[18]. Z. Q. Shi, C. M. Stahle,. and P. Shu, Proc. SPIE, 90, 1998, 3553.

[19]. R. K. Willardson, and A. C. Beer, Semiconductors and Semimetals, 13, 1978, Academic, New York.

[20]. T. E. Schlesinger, and R. B. James, Semiconductors and Semimetals edited **43**, 1995, Academic, San Diego.

[21]. K. Guergouri, M. S. Ferah, R. Triboulet, and Y. Marfaing, J. Cryst.Growth, 6, 1994, 139

[22]. Web-link: http://www.freepatentsonline.com/5528495.

[23]. T. E. Schlesinger, J. E. Toney, H. Yoon, E. Y. Lee, B. A. Brunett, L. Franks and R. B. James, Material Science and Engineering, 32, 2001, 103.

[24]. D. Patidar, K. S. Rathore, N. S. Saxena, K. Sharma, T. P. Sharma, Chalcogenide Letters 5, 2008, 21.

[25]. B. Samanta, S. L. Sharma and A. K. Chaudhuri, Vacuum 46, 1995, 739.

[26]. M. Li and J. C. Li, Materials Letters, 60, 2006, 2526.

[27]. S. Herrera, C. M. Ramos, R. Patino, J. L. Pena, W. Cauich, A. I. Oliva, Brazilian Journal of Physics, 36, 2006 .

[28]. A. Nag, S. Sapra, S. Sen Gupta, A. Prakash, A. Ghangrekar, N. Periasamy, D. Sarma, Bull. Mater. Sci., 31, 2008, 561.

[29]. C. N. R. Rao, G. U. Kulkarni, P. J. Thomas, P. P. Edwards, Chem. Eur. J 8, 2002, 29.

[30]. J. L. Reno, and E. D. Jones, Phys. Rev. 45, 1992, 1440.

[31]. M. Chakraborty, International Journal of Engineering Science and Technology, 3(5), 2011, 3798-3806.

[32]. M. Chakraborty, International Journal of Engineering Science and Technology, 3(10), 2011, 7402-7407.

[33]. M. Chakraborty, International Journal of Engineering Research and Applications, 1(4), 2011, 2096-2104.

[34]. L. A. Kelly, Master of Science thesis, Louisiana State University and Agricultural and Mechanical College, 2005.

[35]. D. J. Wagenaar, K. Parnham, B. Sundal, G. Maehlum, S. Chowdhury, D. Meier, T. Vandehei, M. Szawlowski, B. E. Patt, Advantages of Semiconductor CZT for Medical Imaging, Proc. SPIE. 6707, 2007

[36]. Y. Eisen, I. Mardor, A. Shor et al, IEEE Trans. Nucl. Sci., 49, 2002, 172.

[37]. C. Kittel, Introduction to Solid State Physics, 7th ed, John Willey & Sons, Ch. 3, 1996.

[38]. S. M. Sze, Physics of Semiconductor devices, 2nd ed, Wiley, New York, Ch. 8, 1981.

[39]. B. Ghosh, Applied Surface Science, 254, 2008, 4908-4911.

[40]. B. Ghosh, S. Purakayastha, P. K. Datta, R. W. Miles, M. J. Carter and R. Hill. Semicond. Sci. Technol. 10, 1995, 71-76.

[41]. B. Ghosh, N. K. Mondal, P. Banerjee, J. Pal, and S. Das, IEEE Transactions on Electron Devices, 49(12), 2002, 2352-2355.

[42]. R. W. Miles, B. Ghosh, S. Duke, J. R. Bates, M. J. Carter, P. K. Datta, and R. Hill, Journal of Crystal Growth, 161, 1996, 148-152